*Inorg. Chem.* **2007**, *46*, 9961–9967


# Effects of Water Uptake on the Inherently Oxygen-Deficient Compounds $Ln_{26}O_{27}\square(BO_3)_8$ (Ln = La, Nd)

**Samuel Noirault, Stéphane Célérier, Olivier Joubert, Maria Teresa Caldes, and Yves Piffard***

*CNRS, Université de Nantes, Nantes Atlantique Universités, Institut des Matériaux Jean ROUXEL, UMR n° 6502, 2, rue de la Houssinière, BP 32229-44322 Nantes Cedex 3, France*

Received May 31, 2007

The inherently oxygen-deficient compounds $Ln_{26}O_{27}\square(BO_3)_8$ (Ln = La, Nd) react with water vapor leading to $Ln_{26}O_{26}(OH)_2(BO_3)_8$ phases, and this reaction is reversible. The crystal structure of $Nd_{26}O_{27}\square(BO_3)_8$ has been determined from single-crystal data (space group $P\bar{1}$ with $a = 6.7643(10)$ Å, $b = 12.663(2)$ Å, $c = 14.271(2)$ Å, $\alpha = 90.553(8)°$, $\beta = 99.778(10)°$, and $\gamma = 90.511(9)°$). It is a triclinic distorted version of the monoclinic structure of $La_{26}O_{27}\square(BO_3)_8$. The $Ln_{26}O_{26}(OH)_2(BO_3)_8$ phases both crystallize in the monoclinic system (space group $P2_1/c$ with $a = 6.7445(4)$ Å, $b = 12.6177(9)$ Å, $c = 14.4947(10)$ Å, and $\beta = 100.168(7)°$ for $Nd_{26}O_{26}(OH)_2(BO_3)_8$ and $a = 6.9130(15)$ Å, $b = 12.896(3)$ Å, $c = 14.792(4)$ Å, $\beta = 99.698(16)°$ for $La_{26}O_{26}(OH)_2(BO_3)_8$), and their crystal structure has been determined from single-crystal data, showing that the hydroxyl groups are localized mainly on one of the oxygen sites at room temperature (RT). For the Nd phases, the change in crystal system can result from two different phenomena depending on the atmosphere, either a phase transformation corresponding to a water uptake under wet conditions (triclinic $Nd_{26}O_{27}\square(BO_3)_8$ at RT → monoclinic $Nd_{26}O_{26}(OH)_2(BO_3)_8$) or a phase transition at ∼300 °C for the anhydrous phase under dry conditions (triclinic $Nd_{26}O_{27}\square(BO_3)_8$ at RT → monoclinic $Nd_{26}O_{27}\square(BO_3)_8$ at $T > 300$ °C). For $Nd_{26}O_{26}(OH)_2(BO_3)_8$, the conductivity measured under wet conditions at 300 °C is $\sigma_{300°C} \approx 0.5 \times 10^{-5}$ S cm$^{-1}$. Due to the dehydration process, the proton contribution to the total conductivity of the Nd phase is no longer observed above 500 °C whereas it was still clearly visible at 600 °C for the La phase.

## 1. Introduction

The ability of some oxides to conduct oxide ions at high temperature is associated with structures exhibiting a random distribution of oxygen vacancies, and there are two main classes of such oxides, doped and inherently defective compounds.[1]

A number of these oxygen-deficient oxides have been found to dissolve significant amounts of protons by contact with water vapor and this reaction can be followed under equilibrium conditions by thermogravimetric (TG) analysis. In fact, this reaction can occur during synthesis when samples of these oxides are cooled in ambient air. The incorporation of water involves the filling of oxygen vacancies and the replacement of their effective positive charge by protons as hydroxide ions. Consequently, these oxides can show proton conduction at intermediate or elevated temperature.[2−5]

In this paper, we analyze the effects of water uptake on a new family of inherently defective compounds: the rare-earth oxyborates with $Ln_{26}O_{27}(BO_3)_8$ (Ln = La, Nd) composition. Since the pioneer work of Bartram on rare-earth borates in the 1960s, these borates have been considered as isomorphous $(LnO)_3BO_3$ compounds crystallizing in the $P2_1/c$ monoclinic space group (SG) for Ln = La−Nd.[6] However, recently, the structure of the La phase has been determined, showing that the actual composition of these

* To whom correspondence should be addressed. E-mail: piffard@cnrs-imn.fr.

(1) Norby, T. *J. Mater. Chem.* **2001**, *11*, 11.
(2) Iwahara, H.; Esaka, T.; Uchida, H.; Maeda, N. *Solid State Ionics* **1981**, *3−4*, 359.
(3) Ito, N.; Iijima, M.; Kimura, K.; Iguchi, S. *J. Power Sources* **2005**, *152*, 200.
(4) Norby, T.; Wideroe, M.; Glöckner, R.; Larring, Y. *Dalton Trans.* **2004**, *19*, 3012.
(5) Kreuer, K. D.; Paddison, S. J.; Spohr, E.; Schuster, M. *Chem. Rev.* **2004**, *104*, 4637.
(6) Bartram, S. F. *Proceedings of the 4th Conference on Rare Earth Research*; Eyring, L. R., Ed.; Gordon and Breach, New York, 1965; Section II, pp 165−180.

10.1021/ic701059z CCC: $37.00 
Published on Web 10/11/2007

compounds is not $(LnO)_3BO_3$ but instead $Ln_{26}O_{27}(BO_3)_8$.[7] As nicely described in this latter study, the structure of $La_{26}O_{27}(BO_3)_8$ can be considered as an oxygen-deficient distorted fluorite-type structure. Therefore, the chemical formula of the title compounds can more accurately be written $Ln_{26}O_{27}\square(BO_3)_8$ to illustrate that there is one oxygen vacancy per formula unit. In the La phase, this vacancy is located on the 4e O(13) site on account of its higher atomic displacement parameter (ADP).[7] This is not a clear-cut result, and in any case, the fact that the oxygen vacancy appears as locally disordered does not preclude a larger disorder at higher temperature on other oxygen sites that are bonded only to La (an oxygen vacancy on oxygen sites bonded to B is unlikely). These structural features (oxygen deficiency, fluorite-type structure) prompted us recently to analyze the water uptake and to measure the proton and oxygen ion conductivities of the $La_{26}O_{27}\square(BO_3)_8$ compound.[8] In this contribution, we report on results of similar studies undertaken on the Nd analogue that enable a comparison. In addition we describe the influence of the water uptake on the crystal structures of both La and Nd phases.

## 2. Experimental Section

**Synthesis.** $Ln_{26}O_{27}\square(BO_3)_8$ (Ln = La, Nd) compounds were prepared by solid-state reaction from stoichiometric mixtures of $Ln_2O_3$ and either $B_2O_3$ or $H_3BO_3$ that were heated in Pt crucibles at 1200 °C for 2 days in air. All reactants used were of analytical reagent grade.

**Characterization.** TG analyses were made on a Perkin-Elmer Model TGS-2 TGA system and a Setaram TG-DSC 111 system equipped with a Leybold mass spectrometer (TG-MS).

Wet air was obtained by passing air through a glass tube containing distilled water at 20 °C ($p_{H_2O}$ = 0.023 atm). Dry air was prepared by passing air through a glass tube containing concentrated $H_2SO_4$ (specific gravity: 1.7) and then through another tube containing $P_2O_5$.

**Crystal Structure Determination.** Cell parameters were refined from powder X-ray diffraction (PXRD) patterns (INEL CPS 120 diffractometer, quartz monochromator, Cu K$\alpha$1, $\lambda$ = 1.540598 Å) using the program *FULLPROF*[9] in the Rietveld mode and the *WinPLOTR* interface.[10] All esd values on cell parameters were corrected according to the method proposed by Bérar and Lelann[11] to calculate a reliable estimate of such values.

A Bruker D8 powder diffractometer equipped with an Anton Parr HTK 1200N high-temperature attachment was used to record XRD patterns as a function of temperature up to 950 °C.

Single-crystal data collections were carried out on a Bruker-Nonius Kappa CCD diffractometer (graphite-monochromated Mo K-$L_{2,3}$ radiation). Intensity integration and standard Lorentz-polarization corrections were performed with the Bruker-Nonius *EvalCCD* program package. All other structure calculations were conducted with the *Jana2000* program suite,[12] including corrections for absorption via a Gaussian analytical method.

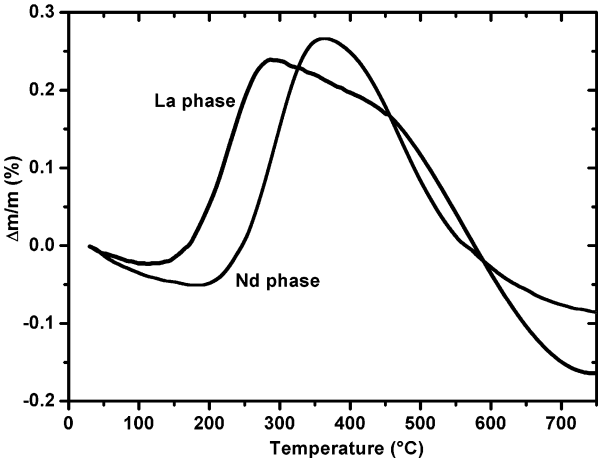


**Figure 1.** TG analysis of the as-prepared La and Nd phases heated at 1 K $min^{-1}$ in wet air.

**Conductivity Measurements.** Conductivity measurements were carried out on samples of the Nd phase pressed in the form of thick pellets (the uniaxial applied pressure was ~6 kbar) and sintered for 48 h at 1300 °C, yielding relative densities of ~95%. A Solartron 1260 high-frequency response analyzer was used with 500 mV of ac perturbation, from 0.1 to 2 MHz, between 300 and 800 °C, in dry and wet ($p_{H_2O}$=0.023 atm) $N_2$. Samples were allowed to equilibrate for 4 h at each temperature. Measurements were also made under deuterated conditions, namely, $N_2$ bubbling in $D_2O$ at 20 °C. Both sides of the pellets were coated with Pt paste acting as electrodes. The complex impedance spectra were analyzed with *Zview* (Scribner Associates, Inc.) and *MicW*[13] electrochemical impedance softwares.

## 3. Results and Discussion

**3.1. Incorporation of Water and Dehydration Behavior.** The purity of the $Ln_{26}O_{27}\square(BO_3)_8$ (Ln = La, Nd) compounds was checked by comparison of the observed XRD patterns with those already reported (JCPDS card number 86-1218 for the La phase and in ref 6 for the Nd phase). In both cases, the agreement is rather fair, with a slight shift of some lines toward low $\theta$ values. For the La phase, it has been shown that this arises as a consequence of a water uptake while being cooled to RT in ambient air.[8] For the Nd phase, a similar explanation is possible; however, this slight shift could also reflect some inaccuracy in the XRD pattern reported for the so-called $(NdO)_3BO_3$ compound.[6] In order to explore this matter further, a ball-milled powder sample of the as-prepared Nd phase was heated at 1K $min^{-1}$ to 800 °C in a TG apparatus under wet air. The TG curve is displayed in Figure 1 along with that recorded previously under similar conditions for the La phase. Both curves show that, as the temperature increases, a weight gain is first observed followed by a weight loss. The rate of weight gain

(7) Lin, J. H.; Su, M. Z.; Wurst, K.; Schweda, E. *J. Solid State Chem.* **1996**, *126*, 287.
(8) Noirault, S.; Célérier, S.; Joubert, O.; Caldes, M.-T.; Piffard, Y. *Adv. Mater.* **2007**, *19*, 867.
(9) Rodríguez-Carvajal, J. *Physica B* **1993**, *192*, 55. See also http://www-llb.cea.fr/fullweb/fp2k/fp2k.htm
(10) Roisnel, T.; Rodríguez-Carvajal, J. *WinPLOTR: a Windows tool for Powder Diffraction Patterns Analysis*; Materials Science Forum, Proc. of the 7th European Powder Diffraction Conference (EPDIC 7); Delhez, R., Mittenmeijer, E. J., Eds.; Trans Tech Publications, Ltd.: Zurich, Switzerland, 2001; Vols. 378−381, pp 118−123. See also http://www-llb.cea.fr/fullweb/winplotr/winplotr.htm.
(11) Bérar, J.-F.; Lelann, P. *J. Appl. Crystallogr.* **1991**, *24*, 1.
(12) Petricek, V.; Dusek, M. *Jana2000, Structure Determination Software Programs*; Institute of Physics: Praha, Czech Republic, 2000.
(13) Suchaud, M. *MicW, a Windows Tool for Measurement and Analysis of Complex Impedance Data*, version 2.0,; Nantes, France, 2004 (contact: michel.suchaud@cnrs-imn.fr).

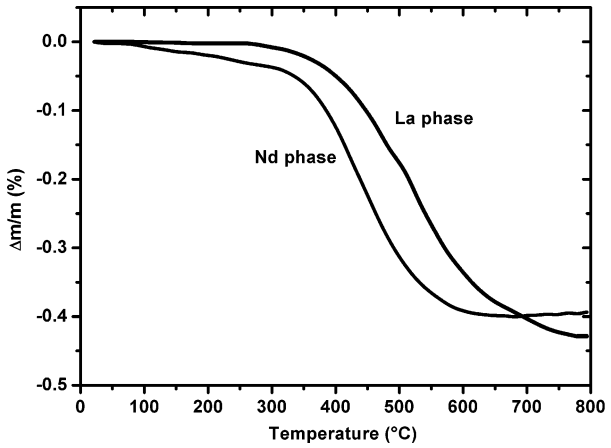


**Figure 2.** TG curves of $Ln_{26}O_{26}(OH)_2(BO_3)_8$ (Ln = La, Nd) phases (heating rate 5 K $min^{-1}$, ambient air).

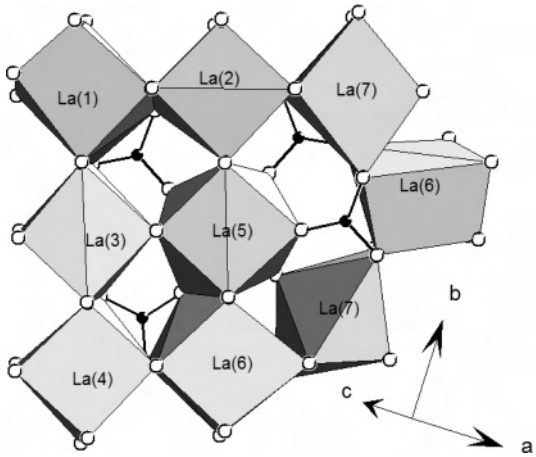


**Figure 3.** View along a direction close to [101] of a fluorite-like layer of $LaO_n$ polyhedra along with the linkage with $BO_3$ groups, in $La_{26}O_{27}\square(BO_3)_8$ (boron and oxygen atoms are represented by black and white circles, respectively).

(Δm/m vs time (at constant heating rate)) reaches its maximum at ∼220 and ∼285 °C, respectively, for the La and Nd phases, then it decreases regularly and the weight gain goes through a maximum at ∼285 and ∼365 °C. The weight gained between RT and this maximum is smaller than the weight lost above this maximum in both cases. This suggests that water was incorporated into the materials during the preparation process; however, due to a too-fast cooling rate of the furnace, the reaction was not complete. Therefore, it proceeds when the sample is further heated in air. Because of the small particle size (<10 $\mu$m) of the powders used in these TG experiments and the rather slow heating rate (1 K $min^{-1}$), the total weight losses recorded between ∼285 and 750 °C (∼0.4%) for the La phase and between ∼365 and 800 °C (∼0.4%) for the Nd phase are in fair agreement with those expected for fully hydrated phases $Nd_{26}O_{26}(OH)_2(BO_3)_8$ (0.385%) and $La_{26}O_{26}(OH)_2(BO_3)_8$ (0.397%). As in the case of the La phase,[8] evidence for the presence of water in the as-prepared Nd sample was given by a TG-MS experiment that proves that the weight loss corresponds to a dehydration process.

Preparation conditions of anhydrous compounds from the as-prepared materials were inferred from the previous TG studies. They include a dehydration treatment at 700 °C for

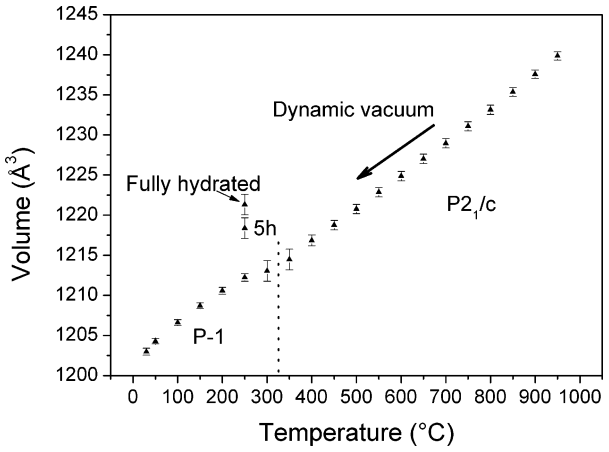


**Figure 4.** Evolution of the unit cell volume of $Nd_{26}O_{27}\square(BO_3)_8$ as a function of temperature under dynamic vacuum (from XRD patterns recorded on cooling) and as a function of time at 250 °C once ambient air pressure was restored.

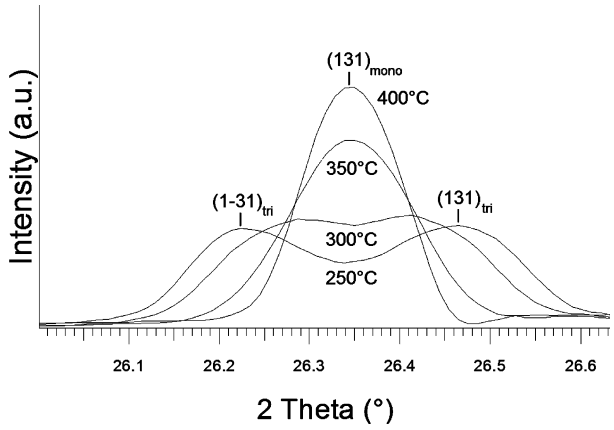


**Figure 5.** Selected part of the XRD powder pattern of $Nd_{26}O_{27}\square(BO_3)_8$, at different temperatures under vacuum, above and below the phase transition.

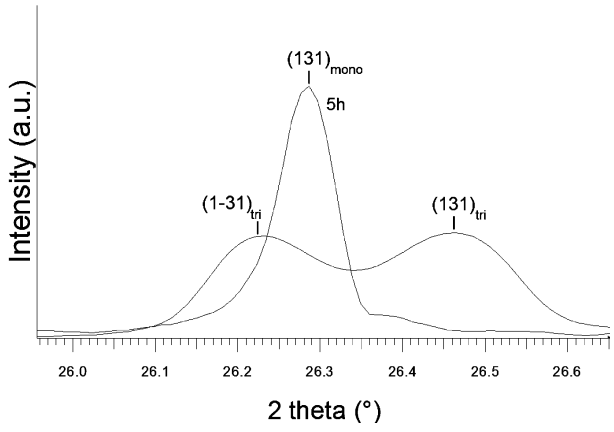


**Figure 6.** Selected part of the XRD powder pattern of the Nd phase at 250 °C as a function of time once the ambient air pressure was restored.

2 h under dynamic vacuum, which is maintained while cooling to RT. A subsequent TG experiment under a dry atmosphere is featureless, thus proving that strictly anhydrous compounds are obtained under such conditions.

The $Ln_{26}O_{26}(OH)_2(BO_3)_8$ (Ln = La, Nd) compounds were prepared from the as-prepared Ln phases upon heating in air at temperatures corresponding to the maximum rate of water uptake, until a steady mass was obtained. Their thermal

**Table 1.** Cell Parameters of $Ln_{26}O_{27}\square(BO_3)_8$ and $Ln_{26}O_{26}(OH)_2(BO_3)_8$ (Ln = La, Nd) Phases[a]

| | $La_{26}O_{27}\square(BO_3)_8$ | $La_{26}O_{26}(OH)_2(BO_3)_8$ | $Nd_{26}O_{27}\square(BO_3)_8$ | $Nd_{26}O_{26}(OH)_2(BO_3)_8$ |
|---|---|---|---|---|
| *a* (Å) | 6.9207(4)<br>*6.920(1)* | 6.9130(15) | 6.7643(10) | 6.7445(4) |
| b (Å) | 12.9204(7)<br>*12.923(1)* | 12.896(3) | 12.663(2) | 12.6177(9) |
| c (Å) | 14.5865(9)<br>*14.571(1)* | 14.792(4) | 14.271(2) | 14.4947(10) |
| α (deg) | | | 90.553(8) | |
| *β* (deg) | 99.353(4)<br>*99.41(1)* | 99.698(16) | 99.778(10) | 100.168(7) |
| *γ* (deg) | | | 90.511(9) | |
| *V* (Å$^3$) | 1287.0(1)<br>*1285.5(2)* | 1299.9(5) | 1204.5(3) | 1214.13(14) |
| SG | $P2_1/c$ | $P2_1/c$ | $P\bar{1}$ | $P2_1/c$ |

[a] For $La_{26}O_{27}\square(BO_3)_8$, values from ref 7 are given in italics for comparison.

behavior illustrated in Figure 2 shows that the water content remains nearly constant up to ~300 °C where it starts to decrease significantly. The fastest dehydration rate is observed at ~400 °C for $Nd_{26}O_{26}(OH)_2(BO_3)_8$ and ~510 °C for $La_{26}O_{26}(OH)_2(BO_3)_8$, and completely anhydrous phases are obtained at ~650 and ~800 °C for the Nd and La compounds, respectively. This higher thermal stability of the hydrated La phase compared with that of the Nd analogue is attributed to its higher basicity (the electronegativity of the $La^{3+}$ cation is smaller than that of $Nd^{3+}$).[14] The total weight losses (0.43 and 0.40%, for the La and Nd compounds, respectively) are in good agreement with those expected for fully hydrated phases.

**3.2. Structural Studies. (a) Description of the Crystal Structure of $La_{26}O_{27}\square(BO_3)_8$.** In the unit cell of $La_{26}O_{27}\square(BO_3)_8$ ($Z = 1$), all atoms are on general position 4e except La(1), which occupies a 2a site.[7] This means that there are 6 La atoms, 13 O atoms, and 2 B atoms occupying 4e sites. If one neglects the oxygen vacancy, La(1), La(4), and La(6) can be considered in a cubic coordination of O atoms whereas La(2), La(3), and La(7) are in a seven-fold coordination, and La(5) adopts a quadratic antiprismatic coordination. The structure of $La_{26}O_{27}\square(BO_3)_8$ can be considered as a distorted version of the fluorite structure. The deviation from the fluorite arrangement is due to the specific geometry of the $(BO_3)^{3-}$ polyanions. This is illustrated in Figure 3 which presents a fluorite-like layer of $LaO_n$ polyhedra along with the linkage with $BO_3$ groups.

**(b) Analysis of the XRD Powder Patterns.** The cell parameters of anhydrous and hydrated Nd phases were refined from XRD powder data. Results are given in Table 1 where they can be compared with those obtained previously for anhydrous and hydrated La phases.[8]

Unexpectedly, though it shows important similarities with that of $La_{26}O_{27}\square(BO_3)_8$, it was not possible to index the powder pattern of $Nd_{26}O_{27}\square(BO_3)_8$ with the use of monoclinic cell parameters. This suggests a triclinic distortion, which is difficult to guess without information from single-crystal data. Therefore, attempts were made to grow single crystals by annealing the prepared powder at 1300 °C in air, and bluish transparent single crystals were obtained. As such, they exhibit a monoclinic unit cell indicating that they likely correspond to a hydrated phase. Consequently, they were further heated at 700 °C under dynamic vacuum for 2 h. Upon this treatment, the crystallinity was maintained and the triclinic distortion was easily detected with the use of a single-crystal diffractometer. That this triclinic distortion was not mentioned in the work of Bartram[6] is not surprising because his material was likely slightly hydrated, and since the structure was not known at that time, he had no specific reason to suspect possible reaction with water vapor during the solid-state synthesis in ambient air.

The powder pattern of $Nd_{26}O_{26}(OH)_2(BO_3)_8$ was successfully indexed with a monoclinic unit cell SG $P2_1/c$) similar to that of $La_{26}O_{26}(OH)_2(BO_3)_8$.[8] Upon hydration, a significant increase of the unit cell volume is observed for both La (12.9 Å$^3$) and Nd phases (9.6 Å$^3$), which is close to the volume of an oxygen atom (~11 Å$^3$). This result agrees with the incorporation of protons filling the oxygen-ion vacancy and forming hydroxide ions, and in Kröger-Vink notation, this can be denoted by

$$H_2O(gas) + V_O^{\bullet\bullet} + O_O^x \rightarrow 2(OH)_O^{\bullet}$$

**(c) From Triclinic $Nd_{26}O_{27}\square(BO_3)_8$ to Monoclinic $Nd_{26}O_{26}(OH)_2(BO_3)_8$.** The change from triclinic $Nd_{26}O_{27}\square(BO_3)_8$ to monoclinic $Nd_{26}O_{26}(OH)_2(BO_3)_8$ raises the following questions: Is that change a consequence of the incorporation of water only (phase transformation)? Could it be the result of a phase transition for the anhydrous phase before the beginning of the incorporation of water? Could it occur in two different ways depending on the atmosphere: (a) only as a consequence of the phase transformation in wet atmosphere (that is, in the absence of a phase transition for the anhydrous phase before the beginning of the incorporation of water) or (b) as a phase transition in dry atmosphere (at a temperature higher than that corresponding to the beginning of the incorporation water)? In order to explore these questions, a thermodiffractometry experiment was undertaken in the following manner. The fully hydrated phase was heated in ambient air at 1 K min$^{-1}$ from RT to 950 °C. At 950 °C, the sample (which corresponds to the anhydrous phase) was placed under dynamic vacuum to avoid any water uptake while cooling and it was cooled down to 50 °C at 1 K min$^{-1}$ in steps of 50 °C. XRD patterns were recorded at

(14) Zhang, Y. *Inorg. Chem.* **1982**, *21*, 3886.

**Table 2.** Crystallographic Data for $Nd_{26}O_{27}\square(BO_3)_8$ and $Ln_{26}O_{26}(OH)_2(BO_3)_8$ Phases

| | $Nd_{26}O_{27}\square(BO_3)_8$ | $Nd_{26}O_{26}(OH)_2(BO_3)_8$ | $La_{26}O_{26}(OH)_2(BO_3)_8$ |
|---|---|---|---|
| | crystal data | | |
| $M_r$ | 4652.7 | 4670.7 | 4532.1 |
| SG | $P\bar{1}$ | $P2_1/c$ | $P2_1/c$ |
| $a$ (Å)[a] | 6.7643(10) | 6.7445(4) | 6.9130(15) |
| $b$ (Å)[a] | 12.663(2) | 12.6177(9) | 12.896(3) |
| $c$ (Å)[a] | 14.271(2) | 14.4947(10) | 14.792(4) |
| α (deg)[a] | 90.553(8) | 90 | 90 |
| $\beta$ (deg)[a] | 99.778(10) | 100.168(7) | 99.698(16) |
| $\gamma$ (deg)[a] | 90.511(9) | 90 | 90 |
| $V$ (Å$^3$) | 1204.5(3) | 1214.13(14) | 1299.9(5) |
| $Z$ | 1 | 1 | 1 |
| $D_x$ (Mg m$^{-3}$) | 6.412 | 6.386 | 5.788 |
| radiation type | Mo Kα | Mo Kα | Mo Kα |
| abs coeff (mm$^{-1}$) | 27.56 | 27.35 | 20.94 |
| cryst size (mm) | 0.015 × 0.023 × 0.063 | 0.01 × 0.039 × 0.094 | 0.045 × 0.061 × 0.082 |
| | data collection | | |
| data collection method | $\omega$, $\phi$ | $\omega$, $\phi$ | $\omega$, $\phi$ |
| $\theta_{max}$ | 40.02 | 40.06 | 40.7 |
| abs corr | gaussian | gaussian | gaussian |
| $T_{min}$, $T_{max}$ | 0.213, 0.674 | 0.171, 0.765 | 0.267, 0.500 |
| reflns collected | 55 552 | 40 846 | 39 160 |
| independent reflns | 14 465 | 7345 | 7981 |
| reflns with $I > 3\sigma(I)$ (obs) | 8718 | 4934 | 5863 |
| | refinement | | |
| no. of vars | 242 | 197 | 197 |
| $R(F)$,[b] $R_w(F)$[c] (obs reflns) | 0.0550, 0.0384 | 0.0433, 0.0248 | 0.0417, 0.0312 |
| $R(F)$,[b] $R_w(F)$[c] (all reflns) | 0.1254, 0.0426 | 0.0889, 0.0275 | 0.0711, 0.0327 |
| $\Delta\rho_{max}$, $\Delta\rho_{min}$ (e$^-$ Å$^{-3}$) (all reflns) | 4.87, −4.79 | 3.94, −4.17 | 4.37, −4.56 |
| extinction method | B-C Lorentzian iso. | B-C Lorentzian iso. | B-C Lorentzian iso. |
| extinction coeff | 0.278(7) | 0.124(6) | 0.395(8) |

[a] Refined from powder data. [b] $R(F) = \sum||F_o| - |F_c||/\sum|F_o|$. [c] $R_w(F) = [\sum w(|F_o| - |F_c|)^2/\sum wF_o^2]^{1/2}$ with $w = 1/[\sigma^2(F_o)]$.

each step during the cooling process, and cell parameters were refined subsequently.

First, this analysis shows that at 950 °C $Nd_{26}O_{27}\square(BO_3)_8$ adopts a monoclinic symmetry. Upon cooling under vacuum, a linear decrease of the monoclinic unit cell volume is observed from 950 to 400 °C (Figure 4). At 350 °C, some monoclinic (*hkl*) peaks start to broaden (Figure 5), giving rise at 300 °C and even more clearly at 250 °C, to pairs of separate triclinic (*hkl*) and (*h*−*kl*) peaks. From 250 °C to RT, a new linear decrease of the triclinic unit cell volume was observed. At this point, the triclinic anhydrous phase was left under vacuum and reheated to 400 °C (above the transition temperature), and a XRD pattern was recorded. It is similar to that recorded at the same temperature upon cooling under vacuum, thus demonstrating the reversibility of this phase transition. Finally, the anhydrous phase was cooled to 250 °C under vacuum, the ambient air pressure was restored, and XRD patterns were recorded subsequently. After 5 h, the XRD pattern is characteristic of a monoclinic phase (Figure 6) with a unit cell volume located in between those of the anhydrous and fully hydrated phases at the same temperature. These results indicate that the initial step of the water uptake is a two-phase reaction inducing a change from triclinic to monoclinic symmetry; then the water uptake proceeds according to a single-phase reaction.

**(d) Single-Crystal Structure Analysis of $Nd_{26}O_{27}\square(BO_3)_8$ and $Ln_{26}O_{26}(OH)_2(BO_3)_8$ (Ln = La, Nd).** The single-crystal structure analyses of both $Nd_{26}O_{27}\square(BO_3)_8$ and $Ln_{26}O_{26}(OH)_2(BO_3)_8$ phases (Ln = La, Nd) were undertaken in order to (1) characterize the triclinic distortion at RT and analyze to which extent the oxygen vacancy is disordered in the anhydrous phase and (2) characterize the hydrated forms of the title materials at RT and try to get some information about location of protons.

Crystals of $Ln_{26}O_{27}\square(BO_3)_8$ were heated in air for several days to obtain the hydrated forms, at 220 and 285 °C for the La and Nd compounds, respectively. Upon this treatment, the crystallinity was maintained and a TG analysis confirmed that the water uptake was maximum.

Crystal characteristics, data collection and reduction parameters, and refinement results are gathered in Table 2.

$Nd_{26}O_{27}\square(BO_3)_8$: Many crystals of the anhydrous phase were tested on the diffractometer, and they all appeared twinned with two nearly overlapping twin domains corresponding to crystals with their pseudomonoclinic *b* axes oriented in opposite directions and nearly coinciding *a* and *c* axes. This type of twinning is likely a consequence of the small deviation of the α and $\gamma$ angles from 90°. A crystal with a small degree of twinning was chosen for the data collection, and the twinning was taken into account in the final refinement, leading to a twin fraction of 0.084(2).

Since the structure is closely related to that of $La_{26}O_{27}\square(BO_3)_8$, starting positional parameters of Nd, O, and B atoms were taken by analogy with those of La, O, and B atoms in this structure.[7] For $Nd_{26}O_{27}\square(BO_3)_8$, there are twice as many atomic positions as in $La_{26}O_{27}\square(BO_3)_8$ because each position of the La phase is split into two nonequivalent positions related by a pseudo $2_1/c$ symmetry in the Nd phase (i.e., ($x$, $y$, $z$) and ∼($x$, $^1/_2 - y$, $^1/_2 + z$)). The atomic positions have been labeled with the same numbers, with the use of prime

**Table 3.** $Ln_{26}O_{26}(OH)_2(BO_3)_8$ (Ln = La, Nd): BVS for the Oxygen Atoms

| atom | BVS in the La phase | BVS in the Nd phase |
|---|---|---|
| O(1) | 1.85(2) | 1.91(2) |
| O(2) | 1.704(18) | 1.84(2) |
| O(3) | 2.010(19) | 2.08(2) |
| O(4) | 1.67(2) | 1.77(2) |
| O(5) | 1.86(2) | 1.81(2) |
| O(6) | 1.759(18) | 1.83(2) |
| O(7) | 2.136(10) | 2.151(11) |
| O(8) | 1.900(9) | 1.892(9) |
| O(9) | 1.511(8) | 1.550(9) |
| O(10) | 2.199(10) | 2.219(11) |
| O(11) | 2.072(10) | 2.094(11) |
| O(12) | 2.073(10) | 2.143(11) |
| O(13) | 2.227(11) | 2.220(11) |

superscripts to take the splitting into account. In addition, inspection of the difference Fourier map suggested that the Nd(6) position must in fact be split into two closely separated sites (Nd(6) and Nd(6″)) about 0.45 Å apart. On the basis of a model imposing equal ADPs for Nd(6) and Nd(6″), the refinement converged to yield an ADP value similar to that of other Nd positions (it was 3−4 times larger for Nd(6) before splitting).

Concerning the location of the oxygen vacancy, oxygen positions O(7) to O(13′) (bonded to Nd only) were first refined as fully occupied, and under this condition, it appeared that the O(13) position exhibited a large ADP ($U_{iso} \sim 0.1$ Å$^2$), much larger than that of other positions O(7) to O(13′). With a site occupancy of 0.5 (required for a composition $Nd_{26}O_{27}\square(BO_3)_8$), the ADP becomes "normal" ($U_{iso} \sim 0.006$ Å$^2$). This result suggests that, as in $La_{26}O_{27}\square(BO_3)_8$, at RT the oxygen vacancy is locally disordered only.

$Ln_{26}O_{26}(OH)_2(BO_3)_8$(Ln = La, Nd): Starting positional parameters of La (Nd), O, and B atoms were also taken by analogy with those of La, O, and B atoms in the structure of $La_{26}O_{27}\square(BO_3)_8$.[7] The structures were refined satisfactorily with the use of this model. In an attempt to locate protons, bond valence sums (BVS) of oxygen atoms were calculated.[15,16] These are listed in Table 3, which shows that one of them is anomalously low (BVS(O(9)) = 1.51 and 1.55, in the La and Nd structures, respectively) compared with the BVS of other oxygen atoms and the expected value of 2. This suggests the presence of one (or several) partially occupied hydrogen site(s) in the environment of O(9) which could interact (hydrogen bonding) with neighboring, slightly underbonded, oxygen atoms O(2), O(4), and O(5) (Figure 7). However, on account of the O−O distances between O(9) and its nearest oxygen neighbors in the La and Nd structures, respectively (O(9)−O(2) = 3.098(5) and 3.007(5) Å, O(9)−O(4) = 2.853(6) and 2.778(6) Å, O(9)−O(5) = 2.937(6) and 2.814(6) Å), this hydrogen bonding remains rather weak. This conclusion agrees with that inferred from the $^1$H magic-angle spinning NMR experiment on the La phase.[8] The difference electron density maps reveal some poorly resolved subsidiary electron density around O(9) in both structures, but the data were deemed inadequate to warrant treatment of H atoms in the refinement (as there are two H atoms per unit cell only, in the most favorable case one would deal with one 4e position that would be half-occupied by protons).

(15) Brese, N. E.; O'Keeffe, M. *Acta Crystallogr.* **1991**, *B47*, 192.
(16) Brown, I. D.; Altermatt, D. *Acta Crystallogr.* **1985**, *B41*, 244.

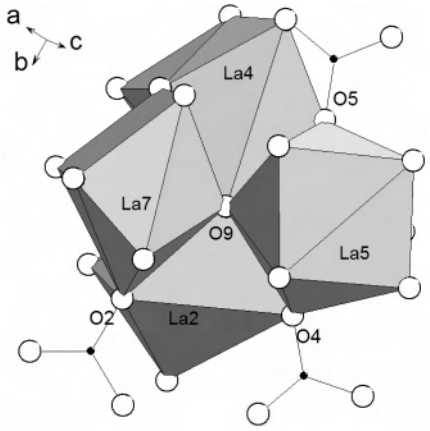


**Figure 7.** Environment of the O(9) atom in $La_{26}O_{26}(OH)_2(BO_3)_8$, showing its nearest oxygen neighbors (O(2), O(4), and O(5)) (boron and oxygen atoms are represented by black and white circles, respectively).

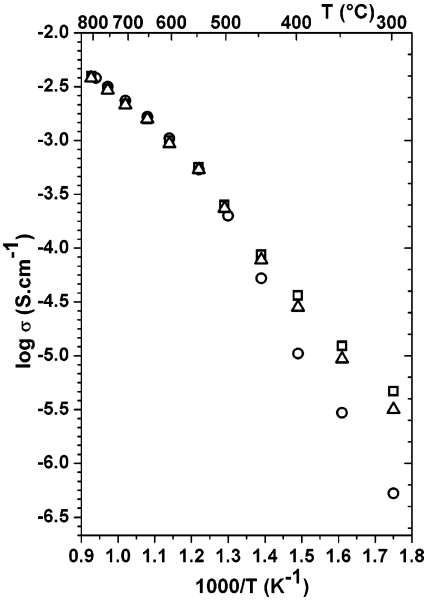


**Figure 8.** Total conductivity as a function of inverse absolute temperature for $Nd_{26}O_{27}\square(BO_3)_8$ under dry (circles) and wet $N_2$ ($p_{H_2O}$ = 0.023 atm (squares)) and $N_2/D_2O$ (triangles).

**3.3. Conductivity Measurements.** To limit the reaction with moisture (in default of being able to avoid it completely) during the sintering process, all pellets were placed in the preheated furnace at ∼400 °C and, upon sintering, removed at the same temperature and allowed to cool to RT in a desiccator containing $P_2O_5$.

Figure 8 shows the conductivity dependence with temperature under dry and wet atmospheres. The data clearly shows a significant increase in the conductivities in wet $N_2$ with respect to the conductivity in dry $N_2$, especially at low temperature. Although the differences are most clearly seen at low temperature, the conductivities in wet $N_2$ remain higher than in dry $N_2$ up to at least 450 °C, suggesting that we are dealing with a proton-conducting material. Further evidence to support the presence of proton conduction is provided by measurements in $N_2/D_2O$ showing a clear H/D isotope effect; an increase in resistance, compared with that

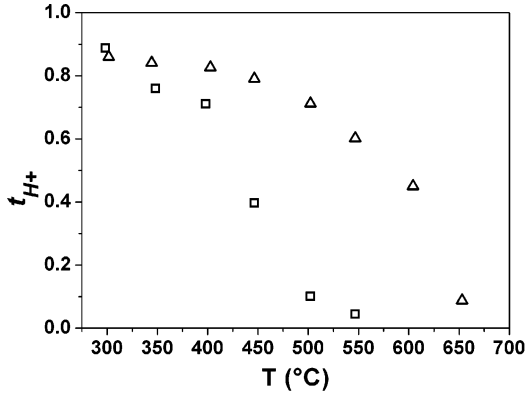


**Figure 9.** Comparison of the proton transference number $t_{H^+}$ (obtained by conductivity measurements) of hydrated La (triangles) and Nd phases (squares).

measured in $N_2/H_2O$, is clearly observed. At temperatures $<500$ °C, the resistance in $N_2/D_2O$ is approximately 1.4 times that in $N_2/H_2O$, in agreement with the expected ratio of $\sqrt{2}$.

On account of the hydration/dehydration behavior described above, the conductivity measured under wet conditions at 300 °C is that of $Nd_{26}O_{26}(OH)_2(BO_3)_8$. Its value ($\sigma_{300°C} \approx 0.5 \times 10^{-5}$ S cm$^{-1}$) is nearly the same as that observed for $La_{26}O_{26}(OH)_2(BO_3)_8$ at the same temperature.[8] At higher temperature, the progressive decrease of the ratio between conductivities in wet and dry conditions is ascribed to a combination of the increase in thermal activation and mobility of the protonic charge carriers and the decrease in their concentration due to the dehydration process. This ratio decreases faster than that in the case of the La phase, in agreement with the higher thermal stability of the hydrated La phase compared with that of the Nd analogue, and the proton contribution to the total conductivity is no longer observed above 500 °C whereas it was still clearly visible at 600 °C for the La phase.[8] Such differences are more clearly reflected by the evolution of the proton transference number $t_{H^+}$ as a function of temperature (Figure 9); $t_{H^+}$ was inferred from conductivity measurements as suggested previously[17] ($t_{H^+} = \sigma_H/\sigma_{wet}$ (with $\sigma_H = \sigma_{wet} - \sigma_{dry}$)).

## 4. Conclusion

When heated in a wet atmosphere, the inherently oxygen-deficient compounds $Ln_{26}O_{27}\square(BO_3)_8$ (Ln = La, Nd) react with water vapor and incorporate protons by filling the oxygen-ion vacancy and forming hydroxide ions, leading to the oxy-hydroxy-borate $Ln_{26}O_{26}(OH)_2(BO_3)_8$. This single-phase reaction is reversible.

$La_{26}O_{27}\square(BO_3)_8$ and $La_{26}O_{26}(OH)_2(BO_3)_8$ both crystallize in the $P2_1/c$ monoclinic SG whereas $Nd_{26}O_{27}\square(BO_3)_8$ and $Nd_{26}O_{26}(OH)_2(BO_3)_8$ crystallize in the $P\bar{1}$ triclinic SG and $P2_1/c$ monoclinic SG, respectively, at RT. This change in crystal system can result from two different phenomena depending on the atmosphere, either a phase transformation corresponding to a water uptake under wet conditions or a phase transition at ~300 °C for the anhydrous phase under dry conditions.

In the crystal structure of $Nd_{26}O_{27}\square(BO_3)_8$ at RT, the oxygen vacancy appears as locally disordered only. The crystal structure determinations of $Ln_{26}O_{26}(OH)_2(BO_3)_8$ (Ln = La, Nd) indicate that, in both structures at RT, the hydroxyl groups are localized mainly on one of the oxygen sites.

$Ln_{26}O_{27}\square(BO_3)_8$ (Ln = La, Nd) compounds are unusual examples of intrinsic oxygen-deficient materials with a crystal structure of low symmetry exhibiting fast proton conduction in wet atmospheres.

**Supporting Information Available:** Tables of final atomic coordinates, site occupancies, and ADPs for $Nd_{26}O_{27}\square(BO_3)_8$ and $Ln_{26}O_{26}(OH)_2(BO_3)_8$ (Ln = La, Nd). This material is available free of charge via the Internet at http://pubs.acs.org. Further details of the crystal structure investigations may be obtained from the Fachinformationszentrum Karlsruhe, 76344 Eggenstein-Leopoldshafen, Germany (fax: (+49)7247−808-666; e-mail: crysdata@fiz-karlsruhe.de) on quoting the deposition numbers CSD-417615 for $Nd_{26}O_{27}\square(BO_3)_8$) and CSD-417613 and 417614 for Nd- and $La_{26}O_{26}(OH)_2(BO_3)_8$, respectively.

IC701059Z

(17) Zhang, G. B.; Smyth, D. M. *Solid State Ionics* **1995**, *82*, 153.